Journal of Robotics and Control (JRC)
Volume 6, Issue 1, 2025
ISSN: 2715-5072, DOI: 10.18196/jrc.v6i2.25990

Design of a Novel Observer-Based SMC for WECS System Using PMSG to Obtain Maximum Energy

Dang Quoc Du [1], Tran Duc Chuyen [2*]
[1, 2] Faculty of Electrical Engineering-Automation, University of Economics - Technology for Industries, Ha Noi, Vietnam
Email: [2] tdchuyen@uneti.edu.vn
*Corresponding Author

***Abstract*—This paper studies and proposes a new sliding mode controller (SMC) for a wind energy conversion system (WECS) using a permanent magnet synchronous wind turbine generator (PMSG) to harvest maximum energy when the wind speed changes. In addition, the paper introduces a nonlinear disturbance observer (NDOB) to estimate the actual wind speed, to provide input to the proposed controller that the authors have studied. The control scheme proposed in this study not only considers the changes in the system parameters, but also considers the randomness of the wind speed changes. The effectiveness of the new SMC design and control scheme is demonstrated by simulation results on Matlab/Simulink software. These results are shown in the change of wind speed deformation, wind deformations that the turbine receives, turbulence assessment, the observer also estimated the non-snow parameters, the system also takes into account maximum power point tracking (MPPT), always consistent with the proposed control law. Moreover, the research results also show that the system works stably, the output is always close to the set value, the system works with high quality, thereby proving that the research results have been studied by the authors are suitable, bringing great benefits in the control process.**

Keywords—Wind Energy Conversion System (WECS); Permanent Magnet Syschronous (PMSG); Sliding Mode Control (SMC); Nonlinear Disturbance Observer (NDOB); Maximum Power Point Tracking (MPPT).

I. INTRODUCTION

The wind energy is a renewable energy source that has been widely used in recent years, because wind is considered a clean and endless source of energy. There have been many different studies and applications to exploit wind energy, in which studies focusing on optimizing the exploitation of wind energy into electricity have been the main trend in recent years both in Vietnam and in the world. The studies that have received much attention are the use of MPPT algorithms for wind turbines, the application of intelligent controllers with control algorithms such as: PID, PI, PD, fuzzy control, adaptive controller, neural networks to estimate parameters, or optimize the power of wind turbines, etc. In wind energy conversion systems (WECS) used in practice, WECS using PMSG are widely used, at that time the system brings many benefits in terms of electrical capacity, and the energy collected is the largest. Because it has many advantages such as high efficiency, low noise, stability and can work with low wind speeds. The MPPT problem applied to WECS is to control the rotational speed of rotor to follow the reference speed of the wind turbine control system, in order to convert wind turbine energy.

In terms of control theory, WECS are highly nonlinear systems, including disturbances, modeling errors and parameters. Therefore, linear controllers are often inefficient and require new, nonlinear and robust controllers, [1]-[5]. Many controllers have been proposed for WECS, In this study, MPPT control is implemented based on the control structure of PMSG. And the MPPT set is also based on VS-WECS set which has been implemented with P&O algorithm with changing processes to optimize the system, [8], [18], [22]. An improved PI controller is proposed for WECS in, [6]-[11]. In [5], model predictive controller (MPC) has also been studied for WECS. The WECS control scheme using Fuzzy algorithm is presented in [6]. Recently, the quadratic linear optimal control (LQ) method has been proposed and proven to be effective for WECS by researchers [7], [8]. The SMC algorithm has been shown to be a capable controller to deal with the problem of nonlinear factors affecting control systems. The feature of SMC is the switching nature of its control action, which provides excellent performance, including the ability to withstand parameter variations, noise factor, and convergence at the end of time. Besides the advantages, SMC also has two major disadvantages. The first is the oscillation factor, caused by the discontinuous control process; the second is related to the inaccurate and unsynchronized control parameters, which seriously degrades the SMC. econd, some of the limitations (disadvantages) of the classic SMC have been improved and upgraded, proven in theory, integrated into Matlab software, Several types of SMC have been successfully applied to WECS in [9], [10]. Although the performance of the conventional SMC algorithm in practical applications is always satisfactory to the controller. But in fact, there are still some disadvantages, such as being susceptible to system measurement noise, difficult to achieve stability when there is inappropriate noise, generating unnecessary large control signals to overcome the problem of parameter nonlinearity, and the most serious is related to high-frequency oscillation due to the intermittent switching control during the system operation, [12]-[19].

For the MPPT algorithm for WECS, the blade tip speed ratio (TSR) method of the wind turbine is commonly used. However, with TSR need information about the actual wind speed is required to be provided to the controller. Cup anemometers are commonly used to measure the actual wind speed fed into the wind turbine, but in some cases it does not guarantee the required accuracy. A method that has been focused on recently is to use observers to estimate the wind speed. In authors, a wind power prediction method was proposed using physical and statistical models, Kalman and Kolmogorov–Zurbenko filters were used to apply local area characteristics and eliminate possible systematic errors, [5], [12]. In recent studies, an adaptive Kalman filter was developed and applied to forecast 2-meter with speed of 10 m/s, the wind speed is considered in the working region allowing the power converter to work normally. The presented method involves adding two strategies to the conventional Kalman filter algorithm to adaptively estimate individual disturbance statistics, aerodynamic torque, and thus estimate the actual wind speed, but the performance of the Kalman filter methods has not been as good as expected, [20]-[28]. A support vector machine model based on genetic algorithm is applied to estimate the wind speed, but the method requires a large amount of data and is computationally complex. Therefore, this paper proposes a turbulence observer for WECS to estimate the aerodynamic torque on the turbine shaft and thus estimate the wind speed fed into the turbine [29]-[36].

In this paper, a NDOB - based SMC is introduced for WECS. Firstly, the dynamic equations of WECS and PMSM generators are built. Since the aerodynamic torque cannot be measured, system dynamics seems to include a disturbance in the drive control system, [37]-[46]. After converting the kinetic energy value into a suitable value for performing the NDOB - based SMC is designed. The NDOB - based SMC method has the following advantages: the nonlinear uncertainty in this technique does not need to satisfy the standard constraint condition H_∞; The gain parameter switching process needs to be higher than the noise estimation error limit, this will then provide computational values that optimize the energy process for wind turbines [47]-[55]. The nominal performance will be maintained because the NDOB calculator acts as a calculation, compensating the loss parameters for the controller and almost not causing any unwanted negative impact on the system when there is a nonlinear uncertainty factor that the NDOB calculator performs parameter estimation to provide full information to the electric drive system controller, [56]-[61]. Furthermore, the final advantage is that the controller has a clear performance advantage since the reduction of measurement uncertainty, in In addition, system stability methods are often achieved by trading off the control performance of the system (this was done in the past, but now there are many measures with many control methods with many newer algorithms such as reinforcement learning in automatic control), [62]-[68]. When we consider the nature of the random wind speed region, the simulation results of the algorithm have been compared and verified to demonstrate the feasibility of the control law that the authors proposed in part three (in this paper), as well as the superiority of its performance value compared to some other conventional control methods, the algorithm we proposed NDOB and SMC always meets the control quality for the system, [69]-[72]. From there to improve the quality of control for this PMSG wind generator system, bringing maximum power energy to the system to help the system optimize the energy process to bring high economic efficiency, [73]-[80].

II. THE BUILDING WECS KINEMATIC MODEL

A. *Wind Turbine Model for the System*

First, From the analysis of the research objectives, we build a dynamic model for the system using a sliding mode controller based on the use of a nonlinear disturbance observer for the WECS system shown in Fig. 1.

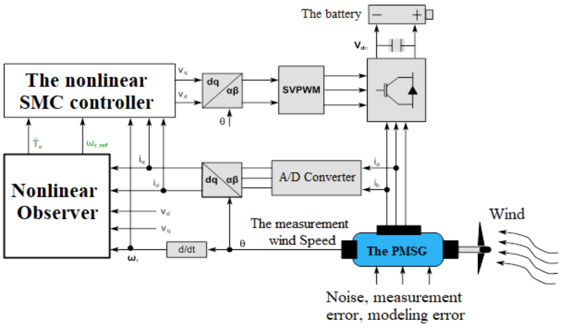

Fig. 1. Sliding control diagram based on a nonlinear disturbance observer for WECS

The aerodynamic power obtained on the wind turbine shaft is represented by the following equation as follows:

$$P_a = \frac{1}{2}\rho\pi R_t^2 C_p(\lambda,\beta)v^3 \tag{1}$$

Where, value ρ is the air density (m/s); component R is the radius of the wind turbine blades (WT) (m); value v is the wind speed (m/s) and the power coefficient $C_p(\lambda,\beta)$ represents the efficiency of the turbine to convert the kinetic energy of the wind into mechanical energy. The value β of this parameter always depends on the shape and size of the wind turbine and it is always a non-linear function of the pitch angle of the wind turbine blades of the PMSG wind turbine. Ingredient β and the tip speed ratio $\lambda = \omega_t R/v$, whereis ω_t the angular speed of the turbine shaft (rad/s). The coefficient C_p usually determined experimentally, this value is provided by the manufacturer (printed on the machine label).

According to formula (1), the power output is increased linearly to the coefficient C_p, which is maximized at the optimal tip speed ratio λ_{opt}. For a given wind turbine, λ_{opt} is a constant value. Therefore, the maximum power output can be achieved by tracking towards the optimal value of rotor speed given by:

$$\omega_{t,ref} = \frac{\lambda_{opt}}{R}v \tag{2}$$

Typically, there are four operating regions for the WT speed to vary depending on the wind speed. For wind speeds below a given threshold, Region I, the wind is not strong enough to move the blades. The second region, Region II, known as the partial load region, which drives the wind turbine, lies between the cut-off region v_{cut-in} and the rated region v_{rate}. The control objective in this region is to maximize the power output. In this region, the pitch angle of the blades is usually fixed at an optimum level and the generator speed is controlled to tracking ω_{ref} in (2). The region III, known as the full load region, covers wind speeds from v_{rate} to $v_{cut-out}$. In this region, the turbine must limit the power output to its rated value so that the electrical and mechanical safety loads are not exceeded. In region IV, above the cut-off level v, with turbine must be shut down to avoid damage, so the power output is zero.

We have the relationship between speed and torque of wind turbine written as follows:

$$n_{gb} = \frac{\omega_r}{\omega_t} = \frac{T_a}{T_{gs}} \tag{3}$$

Where, n_{gb} is the transmission ratio of gearbox; value ω_r is the mechanical angular speed, and ingredient T_{gs} is the equivalent aerodynamic torque of the generator.

B. The Building PMSG Model

The kinematic model of PMSG in the reference d_q coordinate system is written by the following equations:

$$\begin{cases} J\frac{d\omega_r}{dt} = -B\omega_r - T_e + \frac{1}{n_{gb}}T_a \\ \frac{di_q}{dt} = -\frac{R_s}{L}i_q - \frac{\psi_m P}{L}\omega_r - P\omega_r i_d + \frac{1}{L}v_q \\ \frac{di_d}{dt} = -\frac{R_s}{L}i_d + P\omega_r i_q + \frac{1}{L}v_d \end{cases} \tag{4}$$

Where, value i_d and i_q are the d-axis and q-axis currents respectively; value v_d and v_q are the d-axis and q-axis voltages, respectively; ingredient T_a is the mechanical torque ($T_a = P_a/\omega_r$); P is the number of pole pairs, R_s is the stator resistance, $L = L_d = L_q$ are the d-axis and q-axis inductances, J is the rotor inertia; B is the viscous friction coefficient; ψ_m is the magnet flux linkage; and T_e is the electromagnetic torque, which is given by:

$$T_e = Ki_q \tag{5}$$

With, $K = 3/2\psi_m P$.

From equations (4) and (5), we have the dynamic equation system of the wind turbine generator written as follows:

$$\begin{cases} \frac{d\omega_r}{dt} = -\frac{B}{J}\omega_r - \frac{1}{J}T_e + \frac{1}{Jn_{gb}}T_a \\ \frac{dT_e}{dt} = -\frac{R_s}{L}T_e - \frac{\psi_m PK}{L}\omega_r - PK\omega_r i_d + \frac{K}{L}v_q \\ \frac{di_d}{dt} = -\frac{R_s}{L}i_d + \frac{P}{K}\omega_r T_e + \frac{1}{L}v_d \end{cases} \tag{6}$$

Next, based on the expressions in (6), nonlinear NDOB-SMC scheme will be designed based on the following assumptions: One is that ω_r, i_q, và (and also T_e), and i_d are measurable; Two is that the wind speed v and the aerodynamic torque T_a are unknown.

III. THE CONTROLLER DESIGN SLIDING MODE CONTROL

Here we study the surface-type PMSG generator, which is a type of electrical machine that is widely used in research engineering for wind turbine generators, to optimize the power as well as the synchronization process to calculate the design for the transmission system.

A. Research on Controller Design Problem

First of all, when designing the control scheme for this wind turbine system, let us convert the dynamic equations in (6) into another form. Then, we set as follows:

$$Kv_q = u_{qff} + u_{qf} \tag{7}$$

Then the second equation of coefficient (6) is rewritten as follows:

$$\frac{dT_e}{dt} = -\frac{R_s}{L}T_e + \frac{1}{L}u_{qf} \tag{8}$$

Where, $u_{qff} = PK\psi_m\omega_r + PK\psi_m\omega_r Li_d$ is the control offset voltage. Next, we set a new variable as follows:

$$b = -\frac{B}{J}\omega_r - \frac{1}{J}T_e \tag{9}$$

Then, the first equation of the system of equations (6) will become:

$$\frac{d\omega_r}{dt} = b + d \tag{10}$$

With, $d = \frac{1}{Jn_{gb}}T_a$

From equations (8) and (10), the derivative of b is expressed as follows:

$$\frac{db}{dt} = -\frac{BR_s}{JL}\omega_r - \left(\frac{B}{J} + \frac{R_s}{L}\right)b - \frac{B}{J}d - \frac{1}{JL}u_{qf} \tag{11}$$

Here, we set: $a_1 = -\frac{BR_s}{JL}$; $a_2 = -\left(\frac{B}{J} + \frac{R_s}{L}\right)$; $a_3 = -\frac{1}{JL}$

Then, (11) is represented as follows:

$$\frac{db}{dt} = a_1\omega_r + a_2 b - \frac{B}{J}d + a_3 u_{qf} \tag{12}$$

From system (6) and equation (12), we re-represent system (6) as follows:

$$\begin{cases} \frac{d\omega_r}{dt} = b + d \\ \frac{db}{dt} = a_1\omega_r + a_2 b - \frac{B}{J}d + a_3 u_{qf} \\ \frac{di_d}{dt} = -\frac{R_s}{L}i_d + \frac{P}{K}\omega_r T_e + \frac{1}{L}v_d \end{cases} \tag{13}$$

Then we define the error dynamics as follows:

$$\tilde{\omega}_r = \omega_r - \omega_{r,ref}; \tilde{b} = b - \dot{\omega}_{r,ref} \tag{14}$$

Therefore, we have the error dynamics equations of the system represented as the following equations:

$$\begin{cases} \frac{d\tilde{\omega}_r}{dt} = \tilde{b} + d \\ \frac{d\tilde{b}}{dt} = a_1\tilde{\omega}_r + a_2\tilde{b} - \frac{B}{J}d + a_3 u_{qf} \\ \frac{di_d}{dt} = -\frac{R_s}{L}i_d + \frac{P}{K}\omega_r T_e + \frac{1}{L}v_d \end{cases} \tag{15}$$

Here the authors make a convention; the PMSG considered in this paper is a surface mount type generator (SPMSG). For this type of generator, the d-axis current is set to zero to optimize the operating conditions. Therefore, the reference coordinate I_d is also chosen to be zero ($I_d = 0$), [23].

B. Design of a New Sliding Mode Controller Based on Uncertain Nonlinear Disturbance Observer

From the system of equations (15), we see that the system includes a disturbance component d. To estimate this disturbance, a nonlinear disturbance observer (NDOB) is presented in [9], [21], [23], [29], [32], [39], [40], [43], [65], [76] as follows:

$$\begin{cases} \dot{z} = -Lp_2(z + Lx) - L(f + p_1 u) \\ \hat{d} = z + lx \end{cases} \tag{16}$$

Where, $x = \begin{bmatrix} \widetilde{\omega}_r \\ \tilde{b} \end{bmatrix}; f = \begin{bmatrix} \tilde{b} \\ a_1\widetilde{\omega}_r + a_2\tilde{b} - \frac{B}{J}d - \ddot{\omega}_{r,ref} \end{bmatrix}; \ u = u_{qf};\ p_1 = \begin{bmatrix} 0 \\ a_3 \end{bmatrix}; p_2 = \begin{bmatrix} 1 \\ 0 \end{bmatrix}; L = \begin{bmatrix} l_1 \\ l_2 \end{bmatrix}$.

Where, A is the noise estimate, z is the auxiliary variable of NDOB, and L is the non-negative gain of the proposed observer for design.

Estimate D from (1), (2), (3) and (10), estimate moment T_a and the reference rotor speed of the generator can be calculated directly by the relationships as follows:

$$\begin{cases} \hat{T}_a = J\hat{d} \\ \widehat{\omega}_{r,ref} = \sqrt{\frac{\hat{T}_a}{k_{opt}}} \end{cases} \tag{17}$$

In which, $k_{opt} = \frac{1}{2}\rho\pi R_t^5 C_{p,max} \frac{1}{n_{gb}^2 \lambda_{opt}^3}$

The selected sliding mode surface, based on the observed turbulence, is written as follows:

$$\begin{cases} \sigma_q = \tilde{b} + \hat{d} + c\widetilde{\omega}_r \\ \sigma_d = i_d \end{cases} \tag{18}$$

In which, $c > 0$ is the selection coefficient.

Then, the SMC law based on the NDOB as follows:

$$\begin{cases} u_{qf} = -\frac{1}{a_3}\begin{pmatrix} a_1\omega_r + a_2 b - \frac{B}{J}\hat{d} - \ddot{\omega}_{r,ref} + \\ +c(\tilde{b} + \hat{d}) + u_{qs} \end{pmatrix} \\ v_d = -L\left(\frac{P}{K}\omega_r T_e + u_{ds}\right) \end{cases} \tag{19}$$

Where, $u_{qs} = k_q sgn(\sigma_q)$; $u_{ds} = k_d sgn(\sigma_d)$ with k_q and k_d being the chosen control coefficients, always > 0 (always positive).

From reference [18], the stability of the system is proven. First, we have the following assumptions:

- Assumption 1: The disturbance d in the system changes slowly.
- Assumption 2: The estimated error, $e_d = d - \hat{d}$, is bounded by $e_d^* = sup_{t>0}|e_d|$.

Consider the following Lyapunov function:

$$V = \frac{1}{2}\left(\sigma_q^2 + \sigma_d^2\right) \tag{20}$$

Then, from the system of numerical equations (18), then consider the derivative of V:

$$\begin{cases} \dot{\sigma}_q = a_1\omega_r + a_2 b - \frac{B}{J}d + a_3 u_{qf} + \frac{d\hat{d}}{dt} + \\ \qquad + c(\tilde{b} + \hat{d}) \\ \dot{\sigma}_d = -\frac{R_s}{L}i_d + \frac{P}{K}\omega_r T_e + \frac{1}{L}v_d \end{cases} \tag{21}$$

Substituting the values of u_{qf} and v_d from the numerical equation system (19) into system (20), we have:

$$\begin{cases} \dot{\sigma}_q = -k_q sgn(\sigma_q) + \left(c - \frac{B}{J}\right)(d - \hat{d}) + \frac{d\hat{d}}{dt} \\ \dot{\sigma}_d = -k_d sgn(\sigma_d) - \frac{R_s}{L}\sigma_d \end{cases} \tag{22}$$

From equation (16), the derivative of the noise $\hat{d}$ is calculated as follows:

$$\frac{d\hat{d}}{dt} = k_e e_d \tag{23}$$

In which, $k_e = L\left(p_2 - \frac{B}{Ja_3}p_1\right)$. Substitute $\frac{d\hat{d}}{dt}$ from equation (23) and substitute into equation (21), we can calculate as follows:

$$\begin{cases} \dot{\sigma}_q = -k_q sgn(\sigma_q) + \left(c + Lp_2 - \frac{B}{J}\right)e_d \\ \dot{\sigma}_d = -k_d sgn(\sigma_d) - \frac{R_s}{L}\sigma_d \end{cases} \tag{24}$$

From equations (20) and (24), we have the derivative of the Lyapunov (CLF) function V, then we can do:

$$\begin{aligned} \dot{V} &= \sigma_q\dot{\sigma}_q + \sigma_d\dot{\sigma}_d \\ &= -k_q|\sigma_q| + \left(c + k_e - \frac{B}{J}\right)e_d\sigma_q - k_d|\sigma_d| - \frac{R_s}{L}\sigma_d^2 \le \\ &\quad -|\sigma_q|\left[k_q + \left(c + k_e - \frac{B}{J}\right)e_d^*\right] - k_d|\sigma_d| - \frac{R_s}{L}\sigma_d^2 \end{aligned} \tag{25}$$

With k_q chosen so that $k_q > \left(c + k_e - \frac{B}{J}\right)e_d^*$, then $\dot{V} < 0$, so the state of the system will be asymptotically close to the sliding surface: $\sigma_q = \sigma_d = 0$. Substituting the condition $\sigma_q = 0$, into (18), we have:

$$\tilde{b} = -c\widetilde{\omega}_r - \hat{d} \tag{26}$$

Combining with equations (15), (16), and (26), we get the following:

$$\begin{cases} \frac{d\widetilde{\omega}_r}{dt} = -c\widetilde{\omega}_r + e_d \\ \dot{e}_d = -Lp_2 e_d + \dot{d} \end{cases} \tag{27}$$

We see that the system has ensured the condition according to the CLF function to be exponentially stable.

Then, based on [19], Lemma in [1], the system in (27) is input-state stable. This implies that the state variables in (16) and the estimated error will be asymptotically close to zero with the control law based on the observed set proposed by the authors in (16), (18) and (19) is appropriate and then the control law always ensures high quality control process.

Thus, to ensure stability, the switching gain k_q must be chosen to satisfy: $k_q > \left(c + k_e - \frac{B}{J}\right) e_d^*$, where e_d is the estimated error problem and is expected to converge to zero. Therefore, the switching gain can be kept much smaller than the gain of traditional SMC or integral calculators [1], [50]-[53], [64], [65], [67], [72], [74].

IV. THE SIMULATION AND DISCUSSION OF THE RESULTS

After building the model and calculating above, in this section the authors will present the research results based on the above studies on the control algorithm based on the observer which has proven to be highly effective, especially in maintaining quality performance, even under many different operating conditions. Simulation methods often use numerical models and numerical methods to analyze and optimize the control system.

A. *The Simulation Data*

From the control algorithm model of PMSG built in the above section. We conduct simulation studies to prove the research results of the proposed algorithm. From the proposed algorithm controller and parameters are given in Table I. All simulation studies are performed using Matlab - Simulink version R2024a. Then the wind speed is selected with average values of 12.13 m/s and a turbulence intensity of 15.23%. This deformation is illustrated in Fig. 2. The power factor C_p is estimated analytically using a function, with $\lambda_{opt} = 8.09$ and $C_{pmax} = 0.3262$, [21]. The controller parameters are presented in Table II.

TABLE I. PARAMETER TABLE FOR WECS

Symbol	Parameter	Value	Unit
P_{rated}	Rated power	5.6	kW
P	Number of Pole Pairs	14	-
R_s	Stator Resistance	0.3676	W
L	Stator Inductance	3.55	mH
ψ_m	Magnet flux linkage	0.2867	V. s/ rad
J	Moment of Inertia	7.856	kg.m^2
B	Viscosity Coefficient	0.002	kg.m^2/s
R	Turbine Rotor Radius	1.84	m
r	Air Density	1.25	kg/m^3

Next, we have Table II which is the parameters and control methods to evaluate the quality of each controller when simulating the system.

TABLE II. CONTROLLER PARAMETERS

No	Parameter	Value
1	NDOB_NSMC	L = [20 0]; c = 50; k_q = 50; k_d = 1;
2	NDOB_SMC	L = [20 0]; c = 50; k_q = 4e5; k_d = 1e^4;
3	NDOB_PID	L = [20 0]; K_I = 50; K_I = 200; K_D = 25;

Author In this paper, the authors used a real wind measuring device (results as shown in Fig. 2) as a database for wind resource assessment and system evaluation.

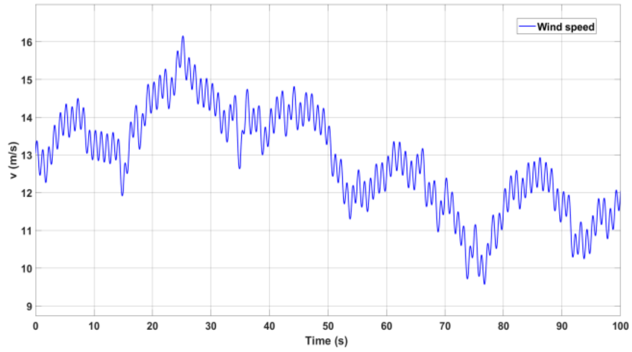

Fig. 2. Actual wind graph taken from a real anemometer

B. *Simulation Results*

From the simulation parameters of the system we have the following results that shown in Fig. 3. From the simulation results of Fig. 3, we can see that: the response value of wind speed always follows the set value. At times 15 seconds and 35 seconds, the wind speed changes little (with v value from 53 to 71 m per second), 55 seconds, 75 seconds, 95 seconds, although the wind speed changes continuously (in accordance with reality), the response value always follows the set value, in the total response time of 100 seconds.

From the simulation results in Fig. 4(a) and Fig. 4(b), the output response value according to the angle always follows the set value, the angle error is very small (about 0.2 rad/s). In Fig. 5(a) and Fig. 5(b), the voltage value achieved has a difference that is consistent with the required response (satisfaction) of the control algorithm. In Fig. 6(a) and Fig. 6(b), the nonlinear error estimate is shown between the SMC controller and the NSMC controller and the PI controller also shows the quality of the controller in the proposed paper to work stably, with high control quality. With Fig. 7(a), although the wind speed changes, the response of the SMC controller still ensures good work in Fig. 7(a), the speed error is small at 0.15m/s, the system works stably Fig. 7(b), the output of the system follows the set value in the equilibrium process, and the control quality is high. The q-axis voltage in case shown in Fig. 8(a), and d-axis voltage shown in Fig. 8(b), for all 3 control methods.

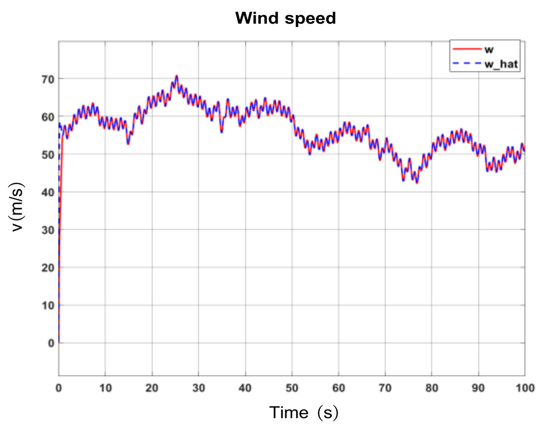

Fig. 3. Response speed ω_r reference speed $\omega_{r,ref}$

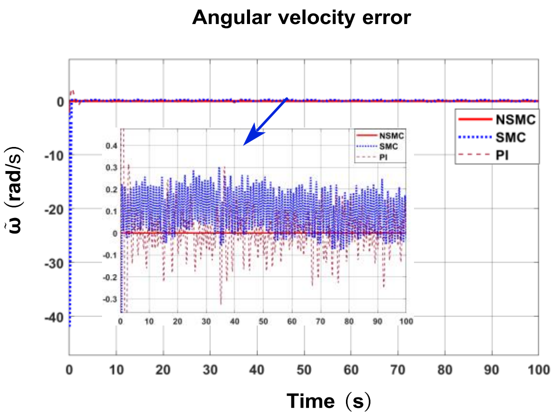

(a)

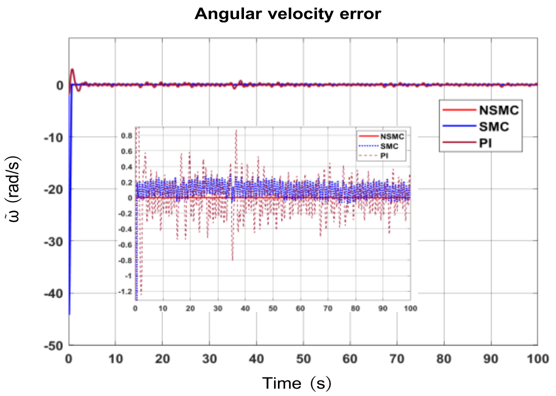

(b)

Fig. 4. Angular velocity deviation $\tilde{\omega}_r$ of the generator rotor for 3 control methods when R, L are rated (figure a) and R increases by 40%, L decreases by 20% (figure b)

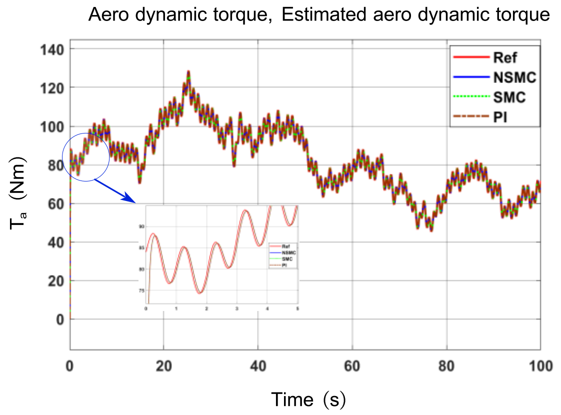

(a)

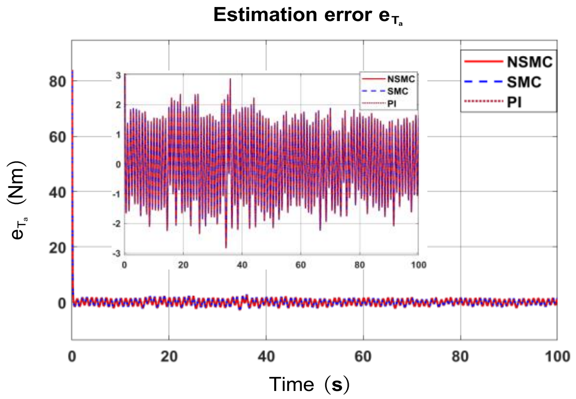

(b)

Fig. 6. Aerodynamic torque T_a and estimated aerodynamic torque $\hat{T}_a$ (figure a), and the error of estimated aerodynamic torque e_{T_a}.

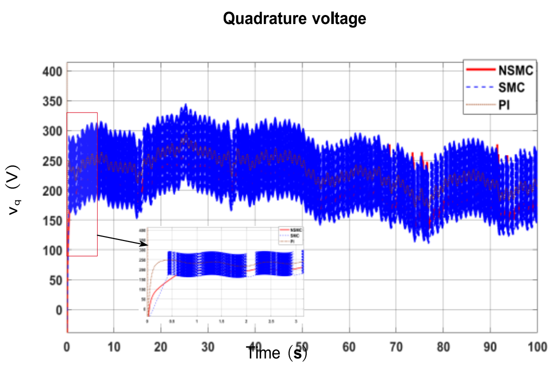

(a)

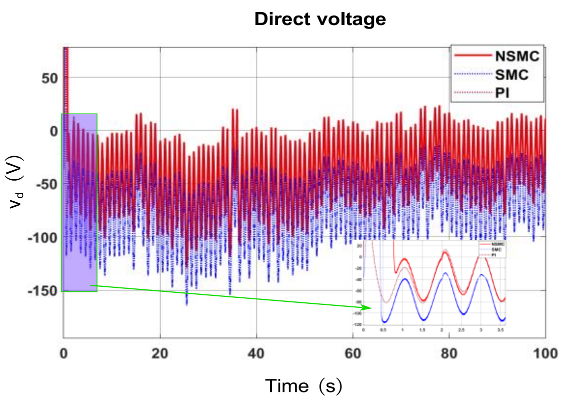

(b)

Fig. 5. Q-axis control voltage and d-axis (figure 5a) voltage for all three control methods (figure 5b)

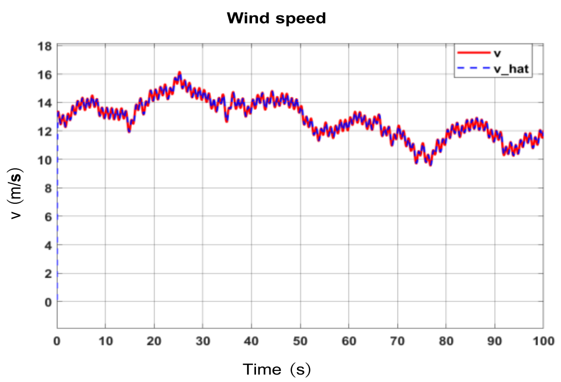

(a)

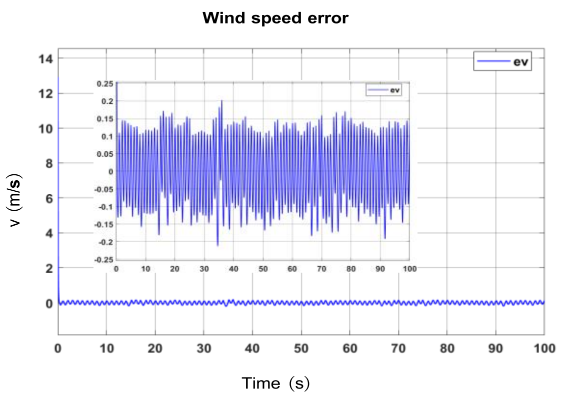

(b)

Fig. 7. Figure 7: shows the wind speed v, estimated wind speed $\hat{v}$ (figure a) and estimated error $e_v = v - \hat{v}$ (figure b)

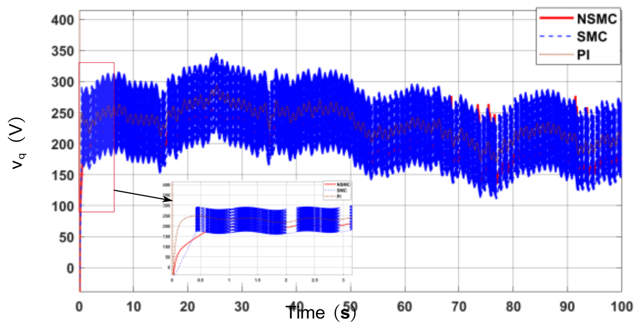

(a)

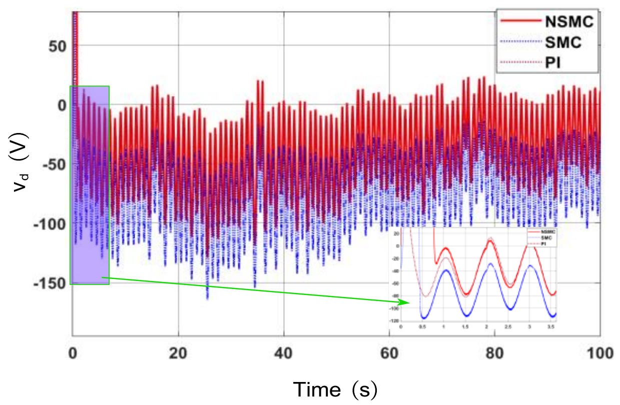

(b)

Fig. 8. The q-axis voltage in case (figure a) and d-axis voltage (figure b), for all 3 control methods

V. CONCLUSION

In this study, an SMC controller is proposed, using the NDOB turbulence observation method for wind energy conversion system without measuring wind speed or aerodynamic torque on the shaft of the wind turbine. With a sliding surface of the SMC control designed, this controller is based on the estimated angular velocity of the PMSG generator rotor, combined with the observed aerodynamic torque disturbance to provide to the controller. The system works with high quality (with the SMC controller and the NDOB controller always meeting the requirements of the calculation process, nonlinear parameter estimation) and is stable even when the wind speed changes at the inlet, the output responses are always stable. The simulation results have demonstrated the performance of the controller and the feasibility of the SMC controller based on this NDOB turbulence observation method. From there, we can affirm that the proposed algorithm is the basis for research, development, calculation, and establishment of control algorithms for wind generators in general or even for electrical drive systems in industry and civil use in general.

ACKNOWLEDGMENT

This research was supported by research foundation funded by Faculty of Electrical - Automation, University of Economics-Technology for Industries, No. 456 Minh Khai Road, Hai Ba Trung district, Ha Noi Capital -Viet Nam National, http://www.uneti.edu.vn/.

REFERENCES

[1] V. Utkin, J. Guldner, and J. Shi, *Sliding Mode Control in Electro-Mechanical Systems*, CRC Press, 2017.

[2] J. Pyrhönen, V. Hrabovcová, and R. S. Semken, Electrical Machine Drives Control: An introduction, *John Wiley & Sons Ltd*, 2016.

[3] IEA, *Key World Energy Statistics*, IEA, 2020.

[4] M. Steinberger, M. Horn, and L. Fridman, *Variable-Structure Systems and Sliding-Mode Control*, Control Engineering: MATLAB Exercises, 2021.

[5] L. Keviczky, R. Bars, J. Hetthéssy, and C. Bányász, *Control Engineering: MATLAB Exercises*, Publishing by Springer Nature Singapore Pte Ltd, USA, 2019, doi: 10.1007/978-981-10-8321-1_1.

[6] H. Wang, P. X. Liu, X. Xie, X. Liu, T. Hayat, and F. E. Alsaadi, "Adaptive fuzzy asymptotical tracking control of nonlinear systems with unmodeled dynamics and quantized actuator," *Information Sciences*, vol. 575, pp. 779-792, 2021.

[7] M. R. Msukwa, E. W. Nshama, and N. Uchiyama, "Adaptive Sliding Mode Control With Feedforward Compensator for Energy-Efficient and High-Speed Precision Motion of Feed Drive Systems," *IEEE Access*, vol. 8, pp. 43571-43581, 2020.

[8] E. M. Youness, "Implementation and validation of backstepping control for PMSG wind turbine using dSPACE controller board," *Energy Reports*, vol. 5, pp. 807-821, 2019.

[9] F. Bakhshande, R. Bach, and D. Söffker, "Robust control of a hydraulic cylinder using an observer-based sliding mode control: Theoretical development and experimental validation," *Control Engineering Practice*, vol. 95, p. 104272, 2020.

[10] Y. Mousavi, A. Zarei, and Z. S. J. Mousavi, "Robust adaptive fractional-order nonsingular terminal sliding mode stabilization of three-axis gimbal platforms," *ISA transactions*, vol. 123, p. 98-109, 2022.

[11] O. Mofid and S. Mobayen, "Robust fractional-order sliding mode tracker for quad-rotor UAVs: event-triggered adaptive backstepping approach under disturbance and uncertainty," *Aerospace Science and Technology*, vol. 146, p. 108916, 2024.

[12] T. D. Chuyen and L. T. T. Hoa, "Improving control quality of win electrical drive system based on intelligent controllers using brushless dc permanent magnet generator," *TNU Journal of Science and Technology*, vol. 226, no. 16, pp. 29-37, 2021.

[13] H. B. Huu, B. D. Thanh, T. D. Chuyen, and V. D. Quoc, "Analytical Comparison of Surface-Mounted Permanent Magnet Synchronous Motors with Inner and Outer Rotor Configurations," *International Journal of Power Electronics and Drive Systems*, vol. 15, no. 4, pp. 2105-2114, 2024.

[14] T. D. Chuyen *et al*., "Improving control quality of PMSM drive systems based on adaptive fuzzy sliding control method," *International Journal of Power Electronics and Drive Systems*, vol 13, no 2, pp. 835-845, 2022.

[15] L. Ovalle, A. Gonzalez, L. Fridman, S. Laghrouche, and H. Obeid, "Analysis of barrier function based adaptive sliding mode control in the presence of deterministic noise," *Automatica*, vol. 171, p. 111946, 2025.

[16] K. A. Alattas *et al*., "Barrier function adaptive nonsingular terminal sliding mode control approach for quad-rotor unmanned aerial vehicles," *Sensors*, vol. 22, no. 3, p. 909, 2022.

[17] M. E. Mahfoud, B. Bossoufi, N. E. Ouanjli, M. Said, and M. Taoussi, "Improved Direct Torque Control of Doubly Fed Induction Motor Using Space Vector Modulation," *International Journal of Intelligent Engineering and Systems*, vol. 14, no. 3, pp. 177-188, 2021.

[18] I. E. Kararoui and M. Maaroufi, "Fuzzy sliding mode power control for wind power generation systems connected to the grid," *International Journal of Power Electronics and Drive Systems*, vol. 13, no. 1, pp. 606-619, 2022.

[19] J. Pande, P. Nasikkar, K. Kotecha, and V. Varadarajan, "A Review of Maximum Power Point Tracking Algorithms for Wind Energy Conversion Systems," *Journal of Marine Science and Engineering*, vol. 9, no. 11, p. 1187, 2021.

[20] B. Majout *et al*., "Improvement of PMSG-Based Wind Energy Conversion System Using Developed Sliding Mode Control," *Energies*, vol. 15, no. 5, p. 1625, 2022.

[21] A. Kashaganova, K. Suleimenov, S. Sagnaeva, and T. D. Do, “Maximum power tracking for wind energy conversion systems via a high-order optimal disturbance observer-based LQR without a wind speed sensor,” *Engineering Science and Technology, an International Journal*, vol. 45, p. 101472, 2023.

[22] A. M. Osman and F. Alsokhiry, "Sliding Mode Control for Grid Integration of Wind Power System Based on Direct Drive PMSG," *IEEE Access*, vol. 10, pp. 26567-26579, 2022.

[23] V. -P. Vu *et al*., "Polynomial Observer-Based Controller Synthesis and Fault-Tolerant Control for Tracking Optimal Power of Wind Energy Conversion Systems," *IEEE Access*, vol. 8, pp. 150130-150141, 2020.

[24] C. D. Cruz-Ancona, L. Fridman, H. Obeid, S. Laghrouche, and C. A. Pérez-Pinacho, “A uniform reaching phase strategy in adaptive sliding mode control,” *Automatica*, vol. 150, p. 110854, 2023.

[25] X. Shen *et al*., "Adaptive Second-Order Sliding Mode Control for Grid-Connected NPC Converters With Enhanced Disturbance Rejection," *IEEE Transactions on Power Electronics*, vol. 37, no. 1, pp. 206-220, 2022.

[26] B. Majout, D. Abrahmi, Y. Ihedrane, C. E. Bakkali, K. Mohammed, and B. Bossoufi, “Improvement of sliding mode power control applied to wind system based on doubly-fed induction generator,” *International Journal of Power Electronics and Drive Systems*, vol. 12, no. 1, pp. 441-452, 2021.

[27] D. Zholtayev, M. Rubagotti, and T. D. Do, “Adaptive super-twisting sliding mode control for maximum power point tracking of PMSG-based wind energy conversion systems,” *Renewable Energy*, vol. 183, pp. 877–889, 2022.

[28] Y. Xie *et al*., “Coupled fractional-order sliding mode control and obstacleavoidance of a four-wheeled steerable mobile robot,” *ISA Transactions*, vol. 108, pp. 282–294, 2021.

[29] R. Shi and X. Zhang, “Adaptive Fractional-order Non-singular Fast Terminal Sliding Mode Control Based on Fixed Time Observer,” *Proceedings of the Institution of Mechanical Engineers, Part C: Journal of Mechanical Engineering Science*, vol. 236, pp. 7006–7016, 2022.

[30] K. Adamiak, “Chattering-Free Reference Sliding Variable-Based SMC,” *Mathematical Problems in Engineering*, vol. 2020, pp. 1–6, 2020.

[31] B. Kharabian and H. Mirinejad, "Hybrid Sliding Mode/H-Infinity Control Approach for Uncertain Flexible Manipulators," *IEEE Access*, vol. 8, pp. 170452-170460, 2020.

[32] T. H. Nguyen, T. T. Nguyen, V. Q. Nguyen, K. M. Le, H. N. Tran, and J. W. Jeon, "An Adaptive Sliding-Mode Controller With a Modified Reduced-Order Proportional Integral Observer for Speed Regulation of a Permanent Magnet Synchronous Motor," *IEEE Transactions on Industrial Electronics*, vol. 69, no. 7, pp. 7181-7191, 2022.

[33] H. Benbouhenni, Z. Boudjema, N. Bizon, P. Thounthong, and N. Takorabet, “Direct Power Control Based on Modified Sliding Mode Controller for a Variable-Speed Multi-Rotor Wind Turbine System Using PWM Strategy,” *Energies*, vol. 15, no. 10, p. 3689, 2022.

[34] J. Ji, S. Jin, W. Zhao, D. Xu, L. Huang, and X. Qiu, "Simplified Three-Vector-Based Model Predictive Direct Power Control for Dual Three-Phase PMSG," *IEEE Transactions on Energy Conversion*, vol. 37, no. 2, pp. 1145-1155, 2022.

[35] X. Zhou, M. Liu, Y. Ma, and S. Wen, "Improved Linear Active Disturbance Rejection Controller Control Considering Bus Voltage Filtering in Permanent Magnet Synchronous Generator," *IEEE Access*, vol. 8, pp. 19982-19996, 2020.

[36] H. E. Aissaoui, A. E. Ougli, and B. Tidhaf, “Neural Networks and Fuzzy Logic Based Maximum Power Point Tracking Control for Wind Energy Conversion System,” *Advances in Science, Technology and Engineering Systems Journal*, vol. 6, pp. 586-592, 2021.

[37] Y. Wang, Y. Zhu, X. Zhang, B. Tian, K. Wang, and J. Liang, "Antidisturbance Sliding Mode-Based Deadbeat Direct Torque Control for PMSM Speed Regulation System," *IEEE Transactions on Transportation Electrification*, vol. 7, no. 4, pp. 2705-2714, 2021.

[38] Y. Wang, Y. Feng, X. Zhang, and J. Liang, "A New Reaching Law for Antidisturbance Sliding-Mode Control of PMSM Speed Regulation System," *IEEE Transactions on Power Electronics*, vol. 35, no. 4, pp. 4117-4126, 2020.

[39] S. Yin and X. Wang, "Super Twisting Control Design for HSPMSG Voltage Stabilization Based on Disturbance Observation Compensation," *IEEE Transactions on Energy Conversion*, vol. 38, no. 2, pp. 1387-1395, 2023.

[40] Q. Hou, S. Ding, and X. Yu, "Composite Super-Twisting Sliding Mode Control Design for PMSM Speed Regulation Problem Based on a Novel Disturbance Observer," *IEEE Transactions on Energy Conversion*, vol. 36, no. 4, pp. 2591-2599, 2021.

[41] Q. Pan, J. Fei, and Y. Xue, "Adaptive Intelligent Super-Twisting Control of Dynamic System," *IEEE Access*, vol. 10, pp. 42396-42403, 2022.

[42] I. Jlassi and A. J. Marques Cardoso, "Enhanced and Computationally Efficient Model Predictive Flux and Power Control of PMSG Drives for Wind Turbine Applications," *IEEE Transactions on Industrial Electronics*, vol. 68, no. 8, pp. 6574-6583, 2021.

[43] T. Li, L. Tao, and B. Xu, “Linear parameter varying observer-based adaptive dynamic surface sliding mode control for PMSM,” *Mathematics*, vol. 12, no. 8, p. 1219, 2024.

[44] K. Ullah, J. Guzinski, and A. F. Mirza, “Critical Review on Robust Speed Control Techniques for Permanent Magnet Synchronous Motor (PMSM) Speed Regulation,” *Energies*, vol. 15, no. 3, p. 1235, 2022.

[45] I. Djelamda and I. Bouchareb, “Field-oriented control based on adaptive neuro-fuzzy inference system for PMSM dedicated to electric vehicle,” *Bulletin of Electrical Engineering and Informatics*, vol. 11, no. 4, pp. 1892-1901, 2022.

[46] C. Xie, J. Wu, Z. Guo, Y. Wang, and J. Liu, “Sensorless control of vehicle-mounted PMSM based on improved sliding mode observer,” *Journal of Physics: Conference Series*, 2021.

[47] K. Mei and S. Ding, "Second-Order Sliding Mode Controller Design Subject to an Upper-Triangular Structure," *IEEE Transactions on Systems, Man, and Cybernetics: Systems*, vol. 51, no. 1, pp. 497-507, 2021.

[48] Z. Liu and W. Chen, “Research on an improved sliding mode observer for speed estimation in permanent magnet synchronous motor,” *Processes*, vol. 10, no. 6, p. 1182, 2022.

[49] H. Yang, J. W. Tang, and Y. R. Chien, “Application of new sliding mode control in vector control of PMSM,” *IEICE Electronics Express*, vol. 19, no. 13, p. 20220156, 2022.

[50] S. Kuppusamy and Y. H. Joo, "Memory-Based Integral Sliding-Mode Control for T–S Fuzzy Systems With PMSM via Disturbance Observer," *IEEE Transactions on Cybernetics*, vol. 51, no. 5, pp. 2457-2465, 2021.

[51] N. Z. Laabidine, B. Bossoufi, I. E. Kafazi, C. E. Bekkali, and N. E. Ouanjli, “Robust Adaptive Super Twisting Algorithm Sliding Mode Control of a Wind System Based on the PMSG Generator,” *Sustainability*, vol. 15, no. 14, p. 792, 2023.

[52] A. Larbaoui, D. E. Chaouch, B. Belabbes, and M. Razkallah, “Application of passivity-based and sliding mode control of permanent magnet synchronous motor under controlled voltage,” *Journal of Vibration and Control*, vol. 28, no. 11-12, pp. 1267–1278, 2022.

[53] P. Zhu, Y. Chen, and M. Li, “Terminal sliding mode control of permanent magnet synchronous motor based on the reaching law,” *Proceedings of the Institution of Mechanical Engineers, Part I: Journal of Systems and Control Engineering*, vol. 234, no. 7, pp. 849-859, 2020.

[54] J. Wang, Y. Wu, C. L. P. Chen, Z. Liu, and W. Wu, “Adaptive PI event-triggered control for MIMO nonlinear systems with input delay,” *Information Sciences*, vol. 677, p. 120817, 2024.

[55] J. Song, Y. -K. Wang, Y. Niu, H. -K. Lam, S. He, and H. Liu, "Periodic Event-Triggered Terminal Sliding Mode Speed Control for Networked PMSM System: A GA-Optimized Extended State Observer Approach," *IEEE/ASME Transactions on Mechatronics*, vol. 27, no. 5, pp. 4153-4164, 2022.

[56] C. Wang, J. Liu, J. Han, Z. Zhang, and M. Jiang, "Analysis of Bidirectional Magnetic Field Modulation on Concentrated Winding Spoke-Type PM Machines," *IEEE Transactions on Transportation Electrification*, vol. 10, no. 3, pp. 6076-6086, 2024.

[57] B. Chen, J. Hu, Y. Zhao, and B. K. Ghosh, “Finite-time observer based tracking control of uncertain heterogeneous underwater vehicles using adaptive sliding mode approach,” *Neurocomputing*, vol. 481, pp. 322–332, 2022.

[58] S. E. Rhaili, A. Abbou, S. Marhraoui, N. E. Hichami, and R. Moutchou, “Optimal Power Generation Control of 5-Phase PMSG Based WECS by Using Enhanced Fuzzy Fractional Order SMC,” *International Journal of Intelligent Engineering and Systems*, vol. 15, no. 2, pp. 572–583, 2022.

[59] N. A. N. Aldin, W. S. E. Abdellatif, Z. M. S. Elbarbary, A. I. Omar, and M. M. Mahmoud, "Robust Speed Controller for PMSG Wind System Based on Harris Hawks Optimization via Wind Speed Estimation: A Real Case Study," *IEEE Access*, vol. 11, pp. 5929-5943, 2023.

[60] J. Tan, K. Zhang, B. Li, and A. -G. Wu, "Event-Triggered Sliding Mode Control for Spacecraft Reorientation With Multiple Attitude Constraints," *IEEE Transactions on Aerospace and Electronic Systems*, vol. 59, no. 5, pp. 6031-6043, 2023.

[61] Q. Rong *et al*., "Asymmetric Sampling Disturbance-Based Universal Impedance Measurement Method for Converters," *IEEE Transactions on Power Electronics*, vol. 39, no. 12, pp. 15457-15461, 2024.

[62] J. Lv, X. Ju, and C. Wang, “Neural network prescribed-time observer-based output-feedback control for uncertain pure-feedback nonlinear systems,” *Expert Systems with Applications*, vol. 264, p. 125813, 2025.

[63] A. Mohammadzadeh, H. Taghavifar, C. Zhang, K. A. Alattas, J. Liu, and M. T. Vu, “A non-linear fractional-order type-3 fuzzy control for enhanced path-tracking performance of autonomous cars,” *IET Control Theory & Applications*, vol. 18, pp. 40-54, 2024.

[64] X. Yu, Y. Feng, and Z. Man, "Terminal Sliding Mode Control – An Overview," *IEEE Open Journal of the Industrial Electronics Society*, vol. 2, pp. 36-52, 2021.

[65] H. Ahn, S. Kim, J. Park, Y. Chung, M. Hu, and K. You, “Adaptive Quick Sliding Mode Reaching Law and Disturbance Observer for Robust PMSM Control Systems,” *Actuators*, vol. 13, no.4, p. 136, 2024.

[66] H. H. H. Mousa, A. R. Youssef, and E. E. Mohamed, “Performance Assessment of Speed Controllers for Five-Phase PMSG with Integrated P&O MPPT Algorithms Based Wind Energy Conversion Systems,” *SVU-International Journal of Engineering Sciences and Applications*, vol. 3, pp. 58–67, 2022.

[67] C. Dang, F. Wang, D. Liu, X. Tong, and W. Song, “Sliding mode predictive control of Vienna rectifier based on optimal vector synthesis,” *Proceedings of the CSEE*, vol. 42, no. 23, pp. 8699-8708, 2022.

[68] K. Mathew K, D. M. Abraham, and A. Harish, “Speed regulation of PMSM drive in electric vehicle applications with sliding mode controller based on harris Hawks optimization,” *e-Prime - Advances in Electrical Engineering, Electronics and Energy*, vol. 9, p. 100643, 2024.

[69] K. Mathew K and D. M. Abraham, “Particle swarm optimization based sliding mode controllers for electric vehicle onboard charger, Comput. Electric,” *Advances in Electrical Engineering*, vol. 96, p. 107502, 2021.

[70] F. Liu, X. Wang, and Z. Xing, "Design of a 35 kW Permanent Magnet Synchronous Motor for Electric Vehicle Equipped With Non-Uniform Air Gap Rotor," *IEEE Transactions on Industry Applications*, vol. 59, no. 1, pp. 1184-1198, 2023.

[71] B. Sarsembayev, K. Suleimenov, and T. D. Do, "High Order Disturbance Observer Based PI-PI Control System With Tracking Anti-Windup Technique for Improvement of Transient Performance of PMSM," *IEEE Access*, vol. 9, pp. 66323-66334, 2021.

[72] X. Liu and H. Yu, “Continuous adaptive integral-type sliding mode control based on disturbance observer for pmsm drives,” *Nonlinear Dynamics*, vol. 104, no. 2, pp. 1429–1441, 2021.

[73] T. Yang, Y. Deng, H. Li, Z. Sun, H. Cao, and Z. Wei, “Fast integral terminal sliding mode control with a novel disturbance observer based on iterative learning for speed control of pmsm,” *ISA Transactions*, vol. 134, pp. 460-471, 2022.

[74] L. Feng, M. Deng, S. Xu, and D. Huang, "Speed Regulation for PMSM Drives Based on a Novel Sliding Mode Controller," in *IEEE Access*, vol. 8, pp. 63577-63584, 2020.

[75] R. Sinha and H. Misra, "Control of PMSM driven Electric Vehicle for Indian Drive Cycle," *2021 National Power Electronics Conference (NPEC)*, pp. 01-06, 2021.

[76] Y. Zhao, X. Liu, H. Yu, and J. Yu, “Model-free adaptive discrete-time integral terminal sliding mode control for PMSM drive system with disturbance observer,” *IET Electric Power Applications*, vol. 14, no. 10, pp. 1756-1765, 2020.

[77] K. Mathew K and D. M. Abraham, “Sliding mode controller with disturbance rejection for bidirectional transformerless ac/dc converter in ev onboard charger,” *Electric Power Components Systems*, vol. 51, no, 14, pp. 1367-1384, 2023.

[78] S. Mishra, A. Varshney, B. Singh and H. Parveen, "Driving-Cycle-Based Modeling and Control of Solar-Battery-Fed Reluctance Synchronous Motor Drive for Light Electric Vehicle With Energy Regeneration," in *IEEE Transactions on Industry Applications*, vol. 58, no. 5, pp. 6666-6675, 2022.

[79] B. Jakovljevi´c, P. Lino, and G. Maione, “Control of double-loop permanent magnet synchronous motor drives by optimized fractional and distributed-order pid controllers,” *European Journal of Control*, vol. 58, pp. 232–244, 2021.

[80] I. Qureshi and V. Sharma, “Analysis of different control schemes of pmsm motor and also a comparison of fopi and pi controller for sensorless msvpwmm scheme,” *e-Prime - Advances in Electrical Engineering, Electronics and Energy*, vol. 6, p. 100359, 2023.